Journal of Alloys and Compounds 504 (2010) 296–302

Contents lists available at ScienceDirect

Journal of Alloys and Compounds

journal homepage: www.elsevier.com/locate/jallcom

First-principles study of the structural, elastic and electronic properties of the anti-perovskites $SnBSc_3$ and $PbBSc_3$

K. Haddadi [a], A. Bouhemadou [a,b,*], L. Louail [a]

[a] Laboratory for Developing New Materials and their Characterization, Department of Physics, Faculty of Science, University of Setif, 19000 Setif, Algeria
[b] Department of Physics and Astronomy, College of Science, King Saud University, P.O. Box 2455, Riyadh 11451, Saudi Arabia

ARTICLE INFO

Article history:
Received 5 February 2010
Received in revised form 26 May 2010
Accepted 28 May 2010
Available online 8 June 2010

PACS:
71.15.Mb
64.30.+t
62.20.Dc
71.20Lp

Keywords:
Anti-perovskite
PP-PW method
Elastic properties
Electronic properties

ABSTRACT

For the first time, the structural, elastic and electronic properties of the scandium-based boride anti-perovskites $SnBSc_3$ and $PbBSc_3$ have been investigated using a first-principles pseudo-potential plane-wave method within the generalized gradient approximation and the local density approximation. The equilibrium lattice constants, bulk moduli and their pressure derivatives, elastic constants, elastic wave velocities, electronic band structures, densities of states and bonding nature are calculated for the single-crystals $SnBSc_3$ and $PbBSc_3$. Pressure dependence of the elastic properties is studied up to 50 GPa. From the anisotropic elastic constants, we have estimated the isotropic elastic parameters and related properties, namely the shear modulus, Young's modulus, Poisson's ratio, Lamé's constants, sound velocities and Debye temperature, for the polycrystalline $SnBSc_3$ and $PbBSc_3$ aggregates.

1. Introduction

The anti-perovskite carbides, nitrides and borides have a wide range of interesting physical and chemical properties, which can be very different depending on the composition [1–3]. The $MC(Mn, Fe)_3$ compounds with M = Al, Ga, In, Ge and d metals, and some related nitrides (e.g., $GaNMn_3$ and $SnNFe_3$) are magnets revealing ferromagnetic, antiferromagnetic, or even more complex types of magnetic ordering and undergoing temperature-driven magnetic phase transition [4–10]. The anti-perovskite nitrides and carbides have received much attention since the discovery of the superconducting properties in $MgCNi_3$ [11]. Intermetallic anti-perovskites closely related to $MgCNi_3$ are therefore subjected to investigations for both the search for new superconductors and the pursuit of a better understanding of the interplay between superconductivity and magnetism. Boron-containing anti-perovskites have been the subject of many experimental and theoretical research work in the last years [1,3,12–26]. Holleck [27] synthesized some cubic anti-perovskite borides Sc-based $ABSc_3$, where A = Sn, Pb, In and Tl. To the best of the authors' knowledge, no information currently exists on the physical properties of $ABSc_3$ compounds, such as elastic and electronic properties. It was suggested that boron-containing anti-perovskites may be good candidates for some technological applications. So, it is timely to investigate some of the not studied physical properties of these materials.

First-principles calculations offer one of the most powerful tools for carrying out theoretical studies of an important number of physical and chemical properties of the condensed matter with great accuracy. It is now possible to explain and predict properties of solids which were previously inaccessible to experiments. Therefore, we think that it is worthwhile to perform first-principles calculations for the structural, elastic and electronic properties of the $SnBSc_3$ and $PbBSc_3$ compounds using the ultra-soft pseudo-potential plane-wave (PP-PW) method in the framework of the density functional theory (DFT) within the generalized gradient approximation (GGA) in order to provide reference data for the theorists and experimentalists for future theoretical and experimental work on this compounds.

This paper is organized as follows. In Section 2, we briefly describe the computational techniques used in this study. The most relevant results obtained for the structural, elastic and electronic properties for the $SnBSc_3$ and $PbBSc_3$ compounds are presented

* Corresponding author at: Laboratory for Developing New Materials and their Characterization, Department of Physics, Faculty of Science, University of Setif, 19000 Setif, Algeria.
E-mail address: a_bouhemadou@yahoo.fr (A. Bouhemadou).

0925-8388/$ – see front matter © 2010 Elsevier B.V. All rights reserved.
doi:10.1016/j.jallcom.2010.05.132

Table 1
Calculated lattice constant a_0 (in Å), bulk modulus B_0 (in GPa) and its pressure derivative B' for $SnBSc_3$ and $PbBSc_3$ compounds; compared with the available experimental data.

	a_0	B_0	B'
$SnBSc_3$			
GGA	4.6145	89.24	3.63
LDA	4.5394	96.24	3.52
Expt. [17]	4.5712		
$PbBSc_3$			
GGA	4.6357	85.64	3.75
LDA	4.5757	92.07	3.72
Expt. [17]	4.622		

and discussed in Section 3. Concluding remarks are given in Section 4.

2. Computational method

Our calculations are performed using *CASTEP* code [28] (Cambridge Serial Total Energy Package), which is an implementation of the pseudo-potential plane-wave method based on the density functional theory (DFT). Interactions of electrons with ion cores were represented by the Vanderbilt-type ultra-soft pseudo-potentials [29] for Sn, Pb, B, and Sc atoms. The electronic exchange–correlation interactions are treated within the recently developed Wu–Cohen generalized gradient approximation (GGA-WC) [30,31] and the local density approximation (LDA), developed by Ceperley and Alder, and parameterized by Perdew and Zunger [32,33]. The cut-off energy for the plane-wave expansion is taken to be 400 eV in all the cases. An $8 \times 8 \times 8$ Monkhorst–Pack mesh [34] is used for the Brillouin-zone integrations.

The structural parameters of $SnBSc_3$ and $PbBSc_3$ are determined using the Broyden–Fletcher–Goldfarb–Shenno (*BFGS*) minimization technique [35]; which provides a fast way of finding the lowest energy structure. The tolerance for geometry optimization is set as the difference of total energy within 5×10^{-7} eV atom^{-1}, maximum ionic Hellmann–Feynman force within 0.01 eV Å^{-1} and maximum stress within 0.02 eV Å^{-3}.

The elastic constants are determined from first-principles calculations by applying a set of given homogeneous deformations with a finite value and calculating the resulting stress with respect to optimizing the internal atomic freedoms [36]. The criteria for convergences of optimization on atomic internal freedoms are selected as the difference of total energy within 1×10^{-6} eV atom^{-1}, ionic Hellmann–Feynman force within 0.002 eV Å^{-1} and maximum ionic displacement within 1×10^{-4} Å. A cubic crystal has three different symmetry elements (C_{11}, C_{12} and C_{44}). One strain pattern, with non-zero first and fourth components, gives stresses related to all three independent elastic constants for the cubic system. Three positive and three negative amplitudes are used for each strain component with the maximum value of 0.5%, and then the elastic stiffness coefficients were determined from a linear fit of the calculated stress as a function of strain.

3. Results and discussion

3.1. Structural properties

The equilibrium lattice constants (a_0), as obtained from the zero-pressure geometry optimization using both GGA and LDA, are presented in Table 1. The calculated lattice constants are in excellent agreement with the available experimental data. The lattice constants calculated using the GGA are higher than the measured ones by only 0.95% and 0.30% for $SnBSc_3$ and $PbBSc_3$, respectively. The LDA approximation underestimates the lattice constants by only 0.70% and 1.0% for $SnBSc_3$ and $PbBSc_3$, respectively. The bulk moduli (B_0) and their pressure derivatives (B') are calculated by fitting the pressure–volume data to a third-order Birch–Murnaghan equation of state (*EOS*) [37] (Fig. 1). We notice here the absence of theoretical and experimental data for the bulk modulus and its pressure derivative in the literature for these two compounds. The calculated bulk modulus value of $SnBSc_3$ is slightly higher than that of $PbBSc_3$.

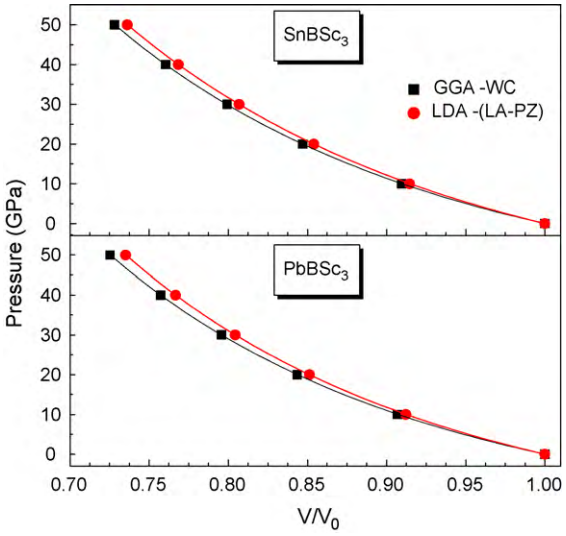

Fig. 1. Calculated pressure–volume relations for the $SnBSc_3$ and $PbBSc_3$ compounds. V_0 is the equilibrium volume. The solid lines are given by the Birch–Murnaghan equation of state with the parameters listed in Table 1.

3.2. Electronic properties

3.2.1. Band structure and density of states

The calculated electronic energy band structures for $SnBSc_3$ and $PbBSc_3$ compounds along the high-symmetry directions in the Brillouin-zone, using the GGA, are shown in Fig. 2. The two studied compounds have nearly similar feature of the electronic band structure and both of them exhibit a metallic character; the valence and conduction bands overlap considerably and there is no band gap at the Fermi level.

The total density of states (TDOS) and atomic site projected local density of states (PDOS) for $SnBSc_3$ and $PbBSc_3$ are depicted in Fig. 3. The overall shape of the TDOS of $SnBSc_3$ is approximately similar to that of $PbBSc_3$. In both compounds, the valence bands characterized by the existence of three separated peaks. The first one is located between −9.0 eV and −6.5 eV (−10.0 eV and −7.5 eV) for $SnBSc_3$ ($PbBSc_3$), and it originates from Sn-5*s* (Pb-6*s*) states. The second peak is situated between −6.4 eV and −4.4 eV (−6.8 eV and −4.4 eV) for $SnBSc_3$ ($PbBSc_3$), and it derives essentially from the B-2*s* states with a minor contribution of the Sn-5*s* (Pb-6*s*) states. The upper part of the valence bands (third peak), that lies from −4.8 eV up to Fermi level, is essentially dominated by Sn-5*p* (Pb-6*p*), B-2*p* and Sc-3*d* states with small contribution from Sc-5*p* (Pb-6*p*) states. The Sn-5*p* (Pb-6*p*) states have nearly the same band width as those of B-2*p*

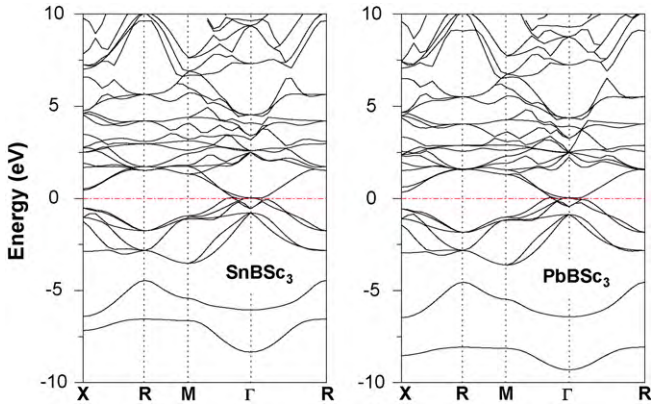

Fig. 2. Band structures along the principal high-symmetry directions in the Brillouin-zone for the $SnBSc_3$ and $PbBSc_3$ compounds.

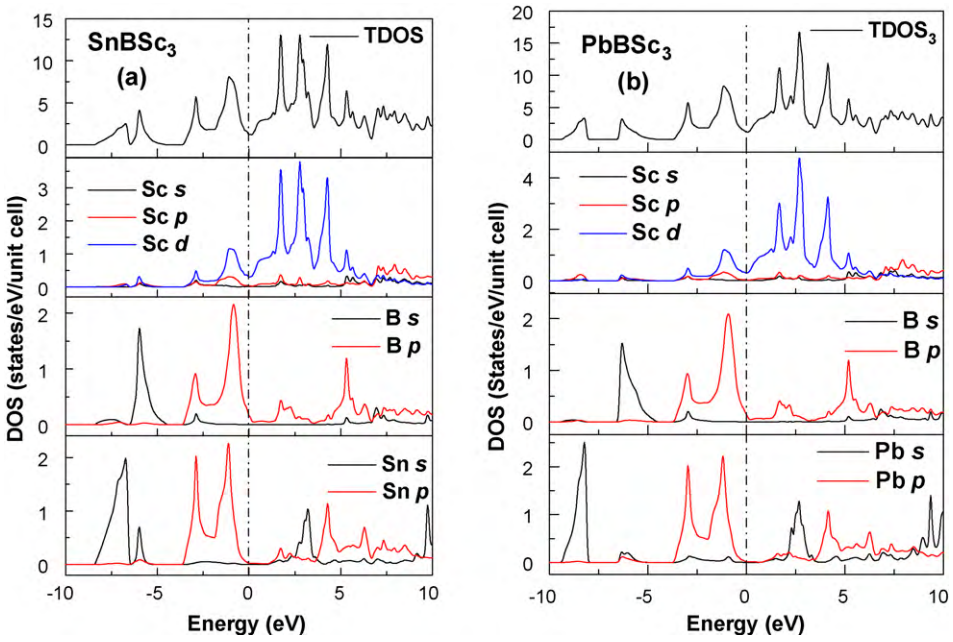

Fig. 3. Calculated total and partial densities of state (TDOS and PDOS, respectively) for the $SnBSc_3$ and $PbBSc_3$ compounds.

and Sc-3*d*, revealing a strong hybridization in this bonding region; indicating a covalent bonding in the studied compounds. At the Fermi level, the density of states is mainly from Sc-3*d* states with minor contribution of B-2*p* states. The bottom of the conduction band is dominated essentially by Sc-3*d* states. The total density of state at the Fermi level $N(E_F)$ is found to be equal to 1.24 and 1.16 states/eV/unit-cell for $SnBSc_3$ and $PbBSc_3$, respectively. Therefore, the electrical conductivity in $SnBSc_3$ would be slightly higher than in $PbBSc_3$.

3.2.2. Mulliken charge population analysis

Table 2 lists the orbital and total charges and the transferred charge of Sn, Pb, B and Sc species. In the two compounds the charge transfers from Sc atom to B and Sn/Pb atoms. For the case of $SnBSc_3$, the transferred charge from Sc to B and Sn are equal to 0.83*e* and 0.84*e*, respectively, while for $PbBSc_3$, the transferred charge from Sc to B and Pb are equal to 0.86*e* and 0.49*e*, respectively. The obtained transferred charge values suggest an effective valence state of $Sn^{-0.83}B^{-0.84}(Sc^{0.56})_3$ and $Pb^{-0.49}B^{-0.86}(Sc^{0.45})_3$.

To provide an objective criterion for bonding nature between atoms, the overlap population may be used to assess the covalent or ionic nature of a bond. Positive and negative bond populations' values indicate bonding and anti-bonding states, respectively. A high value of the bond population indicates a covalent bond, while a low value indicates an ionic interaction [38]. The population ionicity can be calculated from the definition of ionicity scale of He et al. [39] as

$$P_i = 1 - \exp\left(-\frac{P_C - P}{P}\right) \quad (1)$$

where P is the overlap population of a bond and P_C is the bond population for purely covalent bond (here we assume a P_C value equal to 1 as a reperesentative of a purely covalent bond). A population ionicity value P_i equal to 0 indicates a pure covalent bond, while P_i equal to 1 indicates a purely ionic bond. Length, population and population ionicity of the Sn–Sc, Pb–Sc and B–Sc bonds for $SnBSc_3$ and $PbBSc_3$ are given in Table 2. From Table 2, it is clear that, in the two compounds, the B–Sc, the shortest bond, shows a high level of covalency and a low level of ionicity. The Pb–Sc bond in PbBSc3 shows almost a complete ionicity ($P_i \approx 1$).

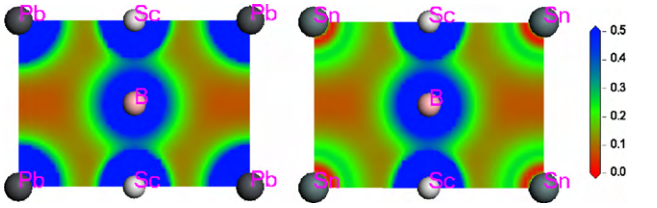

Fig. 4. Valence charge density distribution maps in the (1 1 0) plane for the $SnBSc_3$ and $PbBSc_3$ compounds.

In order to further explore the bonding characteristics in $SnBSc_3$ and $PbBSc_3$, charge density distribution maps in the (1 1 0) plane for these two compounds are plotted and shown in Fig. 4. The figure reveals a sharing of charge between Sc and B due to the Sc-*d* and B-*p* hybridization; thus, there is a covalent bonding between Sc and B. The near-spherical charge distribution around Sn site in the two compounds indicates that the bonding between Pb and Sc and between Sn and Sc are mainly ionic. So there is a bonding anisotropy in the cubic $SnBSc_3$ and $PbBSc_3$ compounds. The bonding character in $SnBSc_3$ and $PbBSc_3$ may be described as a mixture of covalent–ionic and, due to the *d* resonance in the vicinity of the Fermi level, metallic.

3.3. Elastic properties

3.3.1. Elastic constants and elastic wave velocities for the single-crystals $SnBSc_3$ and $PbBSc_3$

The calculated elastic constants for $SnBSc_3$ and $PbBSc_3$, within the LDA and the GGA, are given in Table 3. As we have already mentioned, we are not aware of any experimental or theoretical data for the elastic constants of these two compounds. From Table 3, one can remark that the elastic constants values obtained using the LDA method are higher than those obtained from the GGA method; this can be explained by the fact that the LDA underestimates the lattice constants values compared to the GGA. The unidirectional elastic constant C_{11} values for $SnBSc_3$ and $PbBSc_3$ are about 70% higher than C_{44} values, so these compounds present a relatively weaker resistance to the pure shear deformations. The elastic constants C_{ij} and the bulk modulus values of $SnBSc_3$ are slightly higher

Table 2
Orbital, total and transferred charges of Sn, Pb, B, and Sc atoms, bond length, bond population and population ionicity for $SnBSc_3$ and $PbBSc_3$ compounds, using the GGA-WC method.

	s (e)	p (e)	d (e)	Total (e)	Charge (e)	Bond	Bond length (Å)	Bond populations, P	Population ionicity, P_i
$SnBSc_3$									
B	1.21	2.62	0.00	3.83	−0.83	B–Sc	2.307	0.81	0.209
Sc	2.17	6.62	1.65	10.44	0.56	Sn–Sc	3.263	0.54	0.573
Sn	1.90	2.94	0.00	4.84	−0.84				
$PbBSc_3$									
B	1.21	2.65	0.00	3.86	−0.86	B–Sc	2.318	0.99	0.010
Sc	2.23	6.68	1.64	10.55	0.45	Sc–Pb	3.278	0.00	≈1
Pb	1.53	2.92	10.04	14.49	−0.49				

Table 3
Calculated single-crystals elastic constants (C_{11}, C_{12}, C_{44}), polycrystalline elastic constants (bulk modulus B, shear moduli G, Young's modulus E, Poisson's ratio ν and Lamé's constant λ), Every's anisotropy constant A_E and Zener's anisotropy constant A_Z, for $SnBSc_3$ and $PbBSc_3$ compounds. All constants are in GPa unit except ν, A_E and A_Z which are dimensionless.

	C_{11}	C_{12}	C_{44}	B	G	E	ν	A_E	A_Z	λ
$SnBSc_3$										
GGA	205.7	28.6	63.5	87.7	72.6	170.6	0.176	0.35	0.72	39.3
LDA	224.2	32.0	65.8	96.1	76.6	181.5	0.185	0.38	0.68	45.0
$PbBSc_3$										
GGA	197.1	28.0	61.5	84.3	69.9	164.3	0.175	0.34	0.73	37.7
LDA	211.0	30.8	64.1	90.9	73.5	173.7	0.182	0.35	0.71	41.9

than those of $PbBSc_3$; hence, $SnBSc_3$ is slightly harder than $PbBSc_3$. The consistence between the *EOS* and the elastic properties can be shown by comparing the bulk modulus value estimated from the *EOS*-fitting with that estimated from the calculated elastic constants C_{ij} ($B = C_{11} + 2C_{12}$)/3. The deviation between the two values of B are only about 1.76% (0.17%) and 1.53% (1.29%) for $SnBSc_3$ and $PbBSc_3$, respectively, using the GGA (LDA). This might be an estimate of the reliability and accuracy of the predicted elastic constants for the $SnBSc_3$ and $PbBSc_3$ compounds.

The anisotropic behaviour of a cubic crystal can be measured by the parameter A_E introduced by Every [40] or Zener's ratio A_Z [41]. These two parameters are defined as

$$A_E = \frac{C_{11} - C_{12} - 2C_{44}}{C_{11} - C_{44}} \quad (2)$$

$$A_Z = \frac{2C_{44}}{(C_{11} - C_{12})} \quad (3)$$

For an isotropic crystal $C_{11} - C_{12} = 2C_{44}$, so $A_E = 0$ and $A_Z = 1$. Values of $A_E \neq 0$ and $A_Z \neq 1$, indicate anisotropy. If $A_Z < 1$, the crystal is stiffest along ⟨1 0 0⟩ cube axes, and when $A_Z > 1$ it is stiffest along the ⟨1 1 1⟩ body diagonals [42]. The calculated Every's parameter A_E and Zener's parameter A_Z for $SnBSc_3$ and $PbBSc_3$ using the GGA and the LDA are given in Table 3. We have found that $A_E \neq 0$, $A_Z \neq 1$ and $A_Z < 1$ for the two materials, hence $SnBSc_3$ and $PbBSc_3$ are elastically anisotropic and they are stiffest along ⟨1 0 0⟩ directions.

The elastic behaviour of $SnBSc_3$ and $PbBSc_3$ under pressure effect is investigated for pressure up to 50 GPa. Elastic constants versus pressure are illustrated in Fig. 5. A quadratic pressure dependence of the elastic constants is observed for all constants in the two compounds. All elastic constants increase when the pressure increases. C_{11} is more sensitive to the change of pressure compared to C_{12} and C_{44}. C_{44} increases slightly when the pressure increases. The first- and second-order pressure derivatives of the elastic constants, which present the rate of change as function of pressure, are presented in Table 4.

The elastic constants C_{11}, C_{12} and C_{44} are positive over the considered range of pressure and they satisfy the mechanical stability criteria proposed by Born [43]

$$(C_{11} + 2C_{12} + P) > 0; \quad (C_{44} - P) > 0; \quad (C_{11} - C_{12} - 2P) > 0 \quad (4)$$

Hence, the cubic structure of $SnBSc_3$ and $PbBSc_3$ is mechanically stable.

Using the calculated elastic constants C_{ij}, one can compute the elastic wave velocities in different directions. These parameters are given by the resolution of the Christoffel equation [44]

$$(C_{ijkl} \cdot n_j \cdot n_k - \rho v^2 \delta_{il}) u_l = 0 \quad (5)$$

C_{ijkl} is the single-crystal elastic constant tensor, n is the wave propagation direction, ρ is the density of material, u is the wave polarization and v is the wave velocity. The solutions of this equation are of two types: a longitudinal wave with polarization parallel to the direction of propagation (v_L) and two shear waves (v_{T1} and v_{T2}) with polarization perpendicular to n. The

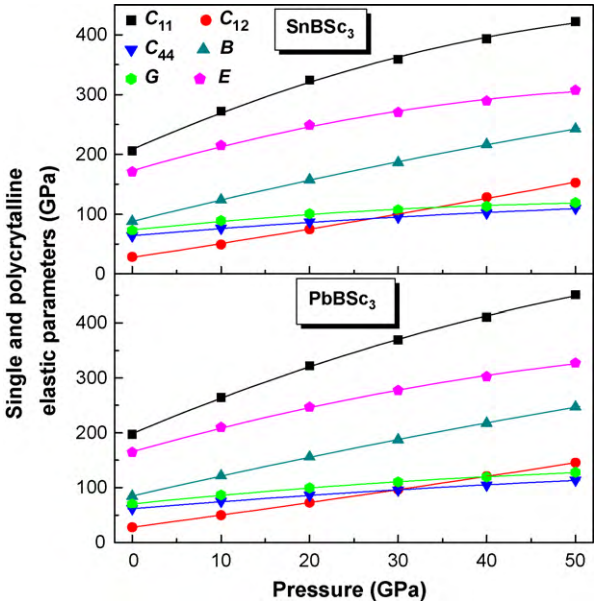

Fig. 5. Calculated pressure dependence of the elastic constants (C_{11}, C_{12} and C_{44}) and isotropic elastic constants (bulk modulus B, shear modulus G, Young's modulus and Lamé's coefficient λ) for the $SnBSc_3$ and $PbBSc_3$ compounds. The solid lines are least-squares second-order polynomial fits of the data points.

Table 4
The calculated first- (α in GPa^{-1}) and second-order (β in 10^{-2} GPa^{-2}) pressure coefficients of the single elastic constants (C_{11}, C_{12} and C_{44}) and polycrystalline elastic constants (B, G, E and λ) for $SnBSc_3$ and $PbBSc_3$ compounds using GGA-WC.

		C_{11}	C_{12}	C_{44}	B	G	E	λ
$SnBSc_3$	α	6.535	2.268	1.241	3.690	1.556	4.342	2.653
	β	−4.601	0.5	−0.684	−1.20	−1.326	−3.39	−0.317
$PbBSc_3$	α	6.807	2.182	1.312	3.724	1.659	4.547	2.618
	β	−3.605	0.333	−0.569	−0.979	−1.04	−2.682	−0.286

Table 5
Elastic waves velocities (in m/s) for different propagation directions for $SnBSc_3$ and $PbBSc_3$ compounds.

		υ_L^{100}	υ_T^{100}	υ_L^{110}	υ_{T1}^{110}	υ_{T2}^{110}	υ_L^{111}	υ_T^{111}
$SnBSc_3$	GGA	6786	3770	6360	3770	4452	6211	4237
	LDA	6911	3744	6427	3744	4524	6258	4280
$PbBSc_3$	GGA	5788	3234	5439	3234	3791	5318	3615
	LDA	5874	3238	5500	3238	3838	5370	3649

calculated elastic wave velocities in [1 0 0], [1 1 0] and [1 1 1] directions for $SnBSc_3$ and $PbBSc_3$ at zero pressure are presented in Table 5.

3.3.2. Elastic parameters and related properties for the polycrystalline $SnBSc_3$ and $PbBSc_3$

In a polycrystalline material, the monocrystalline grains are randomly oriented. On a large scale, such materials can be considered to be quasi-isotropic or isotropic in a statistical sense. An isotropic system is completely described by the bulk modulus B and shear modulus G; these are obtained by a special averaging of the anisotropic elastic constants [45]. There are different schemes of such averaging. For example, one can site the Voigt and Reuss averaging method. The Voigt averaging method is based on the assumption of a uniform strain and the Reuss method is based on the assumption of a homogeneous stress. The former is formulated using the elastic constants C_{ij} and the later using the elastic compliances S_{ij}. Within the Voigt approach, the general expressions for the bulk and shear moduli are [46,47]

$$B_V = \frac{[(C_{11}+C_{22}+C_{33})+2(C_{12}+C_{13}+C_{23})]}{9} \quad (6)$$

$$G_V = \frac{[(C_{11}+C_{22}+C_{33})-(C_{12}+C_{13}+C_{23})+3(C_{44}+C_{55}+C_{66})]}{15} \quad (7)$$

The corresponding expressions within the Reuss approach are

$$B_R = [(S_{11}+S_{22}+S_{33})+2(S_{12}+S_{13}+S_{23})]^{-1} \quad (8)$$

$$G_R = 15[4(S_{11}+S_{22}+S_{33})-4(S_{12}+S_{13}+S_{23})+3(S_{44}+S_{55}+S_{66})]^{-1} \quad (9)$$

For the cubic crystals, $C_{11}=C_{22}=C_{33}$, $C_{12}=C_{12}=C_{23}$, $C_{44}=C_{55}=C_{66}$, and $S_{11}=S_{22}=S_{33}$, $S_{12}=S_{12}=S_{23}$, $S_{44}=S_{55}=S_{66}$.

Using these relations, for the Voigt and Reuss bounds we obtain

$$B_V = \frac{(C_{11}+2C_{12})}{3} \quad (10)$$

$$G_V = \frac{(C_{11}-C_{12}+3C_{44})}{5} \quad (11)$$

and

$$B_R = [3(S_{11}+2S_{12})]^{-1} \quad (12)$$

$$G_R = 5(4S_{11}-4S_{12}+3S_{44})^{-1} \quad (13)$$

Since the cubic elastic compliances may be expressed in terms of the elastic constants as:

$$S_{11}+2S_{12} = (C_{11}+2C_{12})^{-1}$$

$$S_{11}-S_{12} = (C_{11}-C_{12})^{-1} \quad (14)$$

$$S_{44} = (C_{44})^{-1}$$

The Reuss bounds reduce to $B_R = B_V$ and

$$G_R = \frac{5(C_{11}-C_{12})C_{44}}{4C_{44}+3(C_{11}-C_{12})} \quad (15)$$

Hill [48–51] has showed that the Voigt and Reuss bounds are rigorous upper and lower bounds. The average bulk and shear moduli can be estimated from these bounds, e.g., as $B_H = (B_R + B_V)/2$ and $G_H = (G_R + G_V)/2$.

Alternatively, instead of the arithmetic average one might prefer to use the geometric or harmonic means. In weakly anisotropic materials, of course, all these averages lead to similar mean B and G.

The Young's modulus, E, and Poisson's ratio, ν, are connected to B and G by the relations

$$E = \frac{9BG}{3B+G} \quad \text{and} \quad \nu = \frac{3B-2G}{2(3B+G)} \quad (16)$$

The calculated isotropic elastic moduli, namely bulk modulus B, shear modulus G, Young's modulus E, Poisson's ratio ν and Lamé's coefficient λ, for $SnBSc_3$ and $PbBSc_3$ are given in Table 3. It is found that B, G, E and λ values in $SnBSc_3$ are slightly higher than those of $PbBSc_3$, which confirm that $SnBSc_3$ is slightly harder than $PbBSc_3$.

Poisson's ratio ν can formally take values between −1 and 0.5, which corresponds, respectively, to the lower bound where the material does not change its shape and to the upper bound when the volume remains unchanged. For systems with predominantly central interatomic interactions (i.e., ionic crystals), the value of ν is usually close to 0.25 [52]. The $\nu = 0.25$ and 0.5 are the lower limit and the upper limit for central force solids, respectively. This ratio decreases as non-central effects become more important. For covalent materials ν are small ($\nu = 0.1$). In our case, the values of ν are equal to 0.176 (0.185) and 0.175 (0.182) for $SnBSc_3$ and $PbBSc_3$, respectively, from the GGA (LDA) calculation, which means that $SnBSc_3$ and $PbBSc_3$ are affected by a certain amount of non-central forces contributions, indicating a mixed covalent–ionic bonding in these two compounds.

Based on Pugh suggestion [53], which proposes the ratio between the bulk modulus and shear moduli ($B/G = 1.75$) as a criterion to separate the ductile and brittle behaviour of materials (where for $B/G > 1.75$, the material behaves in ductile manner; otherwise, the material behaves in a brittle manner) we have conclude that the two compounds $SnBSc_3$ and $PbBSc_3$ may be classified as brittle materials. The B/G ratio is found to be equal to 1.21 (1.25) and 1.21 (1.24) for $SnBSc_3$ and $PbBSc_3$, respectively, using the GGA

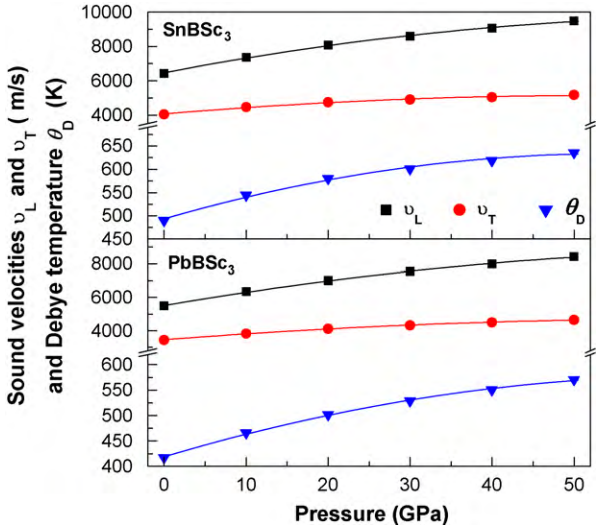

Fig. 6. Longitudinal and transverse **s**ound velocities (υ_L and υ_H, respectively) and Debye temperature (θ_D) versus pressure for the $SnBSc_3$ and $PbBSc_3$ compounds. The solid lines are least-squares second-order polynomial fits of the data points.

(LDA). The more deleterious consequence of brittleness is the sensitivity for thermal shocks, as the material cannot efficiently dissipate thermal stress via plastic deformations. Thus, a brittle solid can only be subjected to limited thermal shocks before its strength drops dramatically.

Furthermore, we have evaluated the effect of the pressure on the isotropic elastic moduli; B, G, E and λ for $SnBSc_3$ and $PbBSc_3$ as it is depicted in Fig. 5. The pressure derivatives of these constants are listed in Table 4. All these parameters increase with increasing pressure, indicating that their hardness increases with pressure.

One of the most important parameter that determines the thermal characteristics of materials is the Debye temperature θ_D. As a rule of thumb, a higher θ_D implies a higher associated thermal conductivity and melting temperature. The knowledge of such a numerical figure is essential for developing and manufacturing electronic devices [42,52]. The Debye temperature (θ_D) of the studied compounds is estimated using the elastic parameters or, more precisely, from the average sound velocity υ_m in term of the following equation [54] (Fig. 6):

$$\theta_D = \frac{h}{k_B}\left[\frac{3n}{4\pi_a}\frac{N_A\rho}{M}\right]^{1/3}\upsilon_m \tag{17}$$

where h is the Planck's constant, k_B is the Boltzmann's constant, n is the number of atoms per molecule, N_A is the Avogadro's number, ρ is the density, M is the molecular weight and υ_m is the average sound velocity. The average sound velocity can be accurately calculated from the elastic constant tensor or using an approximate formula

$$\upsilon_m = \left[\frac{1}{3}\left(\frac{2}{\upsilon_t^3}+\frac{1}{\upsilon_l^3}\right)\right]^{-1/3} \tag{18}$$

where υ_l and υ_t are the longitudinal and transverse sound velocities, respectively. These two parameters can be estimated from the shear modulus G and the bulk modulus B by using the Navier's equation as follow [54]:

$$\upsilon_l = \left(\frac{3B+4G}{3\rho}\right)^{1/2} \quad \text{and} \quad \upsilon_t = \left(\frac{G}{\rho}\right)^{1/2} \tag{19}$$

Results for the density ρ, sound velocities (υ_l, υ_t and υ_m) and Debye temperature θ_D for the $SnBSc_3$ and $PbBSc_3$ compounds are given in Table 6.

Table 6
Density ρ (in g/cm^3), longitudinal, transverse and average sound velocities (υ_l, υ_t and υ_m, respectively, in m/s) (calculated from polycrystalline elastic moduli) and the Debye temperatures (θ_D in K) (calculated from the average sound velocity) for $SnBSc_3$ and $PbBSc_3$ compounds.

	Species	ρ	υ_l	υ_t	υ_m	θ_D
$SnBSc_3$	GGA	4.47	6425.0	4030.3	4438.0	489.9
	LDA	4.69	6498.4	4039.8	4452.8	499.7
$PbBSc_3$	GGA	5.88	5493.5	3446.9	3795.5	417.1
	LDA	6.12	5556.9	3466.5	3819.5	425.2

4. Conclusion

To summarise, for the first time, we have studied the structural, electronic and elastic properties of the cubic anti-perovsite borides Sc-based $SnBSc_3$ and $PbBSc_3$ by using a pseudo-potential plane-wave approach based on the density functional theory within the generalized gradient approximation and the local density approximation. The calculated equilibrium lattice constants agree well with the available experimental data; validating the theoretical method used in this work. The band structures show that the two studied materials are electrical conductors. Mulliken charge population analysis reveals that the bonding in $SnBSc_3$ and $PbBSc_3$ is a mixture of covalent and ionic character. All calculated elastic parameters are found to have quadratic dependence with pressure. The bulk modulus derived from the single elastic constants C_{ij} has nearly the same value as the one estimated from the *EOS*-fitting; this might be an estimate of the reliability and accuracy of the predicted elastic constants for $SnBSc_3$ and $PbBSc_3$ compounds. $SnBSc_3$ and $PbBSc_3$ show an elastic anisotropy. Using the empirical rule of Pugh, we have found that the two compounds can be classified as brittle materials.

References

[1] C. Loison, A. Leithe-Jasper, H. Rosner, Phys. Rev. B 75 (2007) 205135.
[2] A.L. Ivanovskii, A.I. Gusev, G.P. Shveoekin, Quantum Chemistry in Materials Science: Ternary Carbides and Nitrides of Transition Metals and III and V Subgroup Elements, Ural Division, Russian Academy of Sciences, Yekaterinburg, 1996 (in Russian).
[3] T. Shishido, K. Kudou, T. Sasaki, S. Okada, J. Ye, K. Iizumi, A. Nomura, T. Sugawara, K. Obara, M. Tanaka, S. Kohiki, Y. Kawazoe, K. Nakajima, M. Oku, J. Alloys Compd. 383 (2004) 294.
[4] K. Motizuki, H. Nagai, T. Tanimoto, J. Phys. 49 (1998) 8.
[5] M. Shirai, Y. Ohata, N. Suzuki, K. Motizuki, Jpn. J. Appl. Phys. 32 (1993) 250.
[6] S. Ishida, S. Fujii, A. Sawabe, S. Asano, Jpn. J. Appl. Phys. 32 (1993) 282.
[7] C. Kuhnen, A. Dos Santos, Solid State Commun. 85 (1993) 273.
[8] A.L. Ivanovskii, Zh. Neorg. Khim. 41 (4) (1996) 650 (Russ. J. Inorg. Chem. 41 (1996) 650).
[9] A. Dos Santos, C. Kuhnen, J. Alloys Compd. 321 (2001) 60.
[10] V.V. Bannikov, I.R. Shein, A.L. Ivanovskii, Phys. Solid State 149 (2007) 1704.
[11] N. He, Q. Huang, A.P. Ramirez, Y. Wang, K.A. Regan, N. Rogado, M.A. Hayward, M.K. Haas, J.S. Slusky, K. Inumara, H.W. Zandbergen, N.P. Ong, R.J. Cava, Nature 411 (2001) 54.
[12] H. Takei, T. Shishido, J. Less-Common Met. 97 (1984) 223.
[13] T. Shishido, J. Ye, T. Sasaki, R. Note, K. Obara, T. Takahashi, T. Matsumoto, T. Fukuda, J. Solid State Chem. 133 (1997) 82.
[14] C. Felser, J. Alloys Compd. 87 (1997) 262.
[15] T. Shishido, J. Ye, K. Kudo, S. Okada, K. Obara, T. Sugawara, M. Oku, K. Wagatsuma, H. Horiuchi, T. Fukuda, J. Alloys Compd. 291 (1999) 52.
[16] T. Shishido, T. Sasaki, K. Kudou, S. Okada, A. Yoshikawa, J.M. Ko, J. Ye, I. Higashi, M. Oku, H. Horiuchi, T. Fukuda, S. Kohiki, K. Nakajima, J. Alloys Compd. 335 (2002) 191.
[17] T. Shishido, J. Ye, K. Kudou, S. Okada, K. Iizumi, M. Oku, Y. Ishizawa, A. Yoshikawa, M. Tanaka, A. Nomura, T. Sugawara, K. Obara, T. Amano, S. Oishi, N. Kamegashira, Y. Kawazoe, S. Kohoki, K. Nakajuma, J. Alloys Compd. 375 (2004) 217.
[18] M. Oku, T. Shishido, M. Arai, K. Wagatsuma, K. Nakajima, J. Alloys Compd. 390 (2005) 202.
[19] D. Music, Z. Sun, J.M. Schneider, Phys. Rev. B 71 (2005) 052104.
[20] R. Sahara, T. Shishido, A. Nomura, K. Kudou, S. Okada, V. Kumar, K. Nakajima, Y. Kawazoe, Comput. Mater. Sci. 36 (2006) 12.
[21] T. Shishido, Y. Ishizawa, J. Ye, S. Okada, K. Kudou, K. Iizumi, M. Oku, M. Tanaka, A. Yoshikawa, A. Nomura, T. Sugawara, S. Tozawa, K. Obara, S. Oishi, N.

Kamegashira, T. Amano, R. Sahara, V. Kumar, H. Horiuchi, S. Kohiki, Y. Kawazoe, K. Nakajima, J. Alloys Compd. 408–412 (2006) 375.
[22] D. Muzic, R. Ahuja, J.M. Schneider, Phys. Lett. A 356 (2006) 251.
[23] T. Shishido, J. Ye, S. Okada, K. Kudou, K. Iizumi, M. Oku, Y. Ishizawa, R. Sahara, V. Kumar, A. Yoshikawa, M. Tanaka, H. Horiuchi, A. Nomura, T. Sugawara, K. Obara, T. Amano, S. Kohiki, Y. Kawazoe, K. Nakajima, J. Alloys Compd. 408–412 (2006) 379.
[24] H. Kojima, R. Sahara, T. Shishido, A. Nomura, Appl. Phys. Lett. 91 (2007) 081901.
[25] R. Sahara, T. Shishido, A. Nomura, Phys. Rev. B 76 (2007) 024105.
[26] R. Schaak, M. Avdeev, W.-L. Lee, G. Lawes, J. Jorgensen, N. Ong, A. Ramirez, R. Cava, J. Solid State Chem. 177 (2004) 1244.
[27] H. Holleck, J. Less-Common Met. 52 (1977) 167.
[28] M.D. Segall, P.J.D. Lindan, M.J. Probert, C.J. Pickard, P.J. Hasnip, S.J. Clark, M.C. Payne, J. Phys.: Condens. Matter 14 (2002) 2717.
[29] D. Vanderbilt, Phys. Rev. B 41 (1990) 7892.
[30] Z. Wu, R.E. Cohen, Phys. Rev. B 73 (2006) 235116.
[31] F. Tran, R. Laskowski, P. Blaha, K. Schwarz, Phys. Rev. B 75 (2007) 115131.
[32] D.M. Ceperley, B.J. Alder, Phys. Rev. Lett. 45 (1980) 566.
[33] J.P. Perdew, A. Zunger, Phys. Rev. B 23 (1981) 5048.
[34] H.J. Monkhorst, J.D. Pack, Phys. Rev. B 13 (1976) 5188.
[35] T.H. Fischer, J. Almlof, J. Phys. Chem. 96 (1992) 9768.
[36] V. Milman, M.C. Warren, J. Phys.: Condens. Matter 13 (2001) 241.
[37] F. Birch, J. Geophys. Res. B 83 (1978) 1257.
[38] M.D. Segall, R. Shah, C.J. Pickard, M.C. Payne, Phys. Rev. B 54 (1996) 16317.
[39] J. He, E. Wu, H. Wang, R. Liu, Y. Tian, Phys. Rev. Lett. 94 (2005) 015504.
[40] A.G. Every, Phys. Rev. B 22 (1980) 1746.
[41] C. Zener, Elasticity and Anelasticity of Metals, University of Chicago Press, Chicago, 1948.
[42] R.E. Newnham, Properties of Materials; Anisotropy, Symmetry, Structure, Oxford University Press, New York, 2005.
[43] M.J. Mehl, B.M. Klein, in: J.H. Westbrook, R.L. Fleischeir (Eds.), Papaconstantopoulos, Intermetallic Compounds: Principle and Practice, Vol. I: Principles, John Wiley and Sons, London, 1995.
[44] B.B. Karki, L. Stixrude, S.J. Clark, M.C. Warren, G.J. Ackland, J. Crain, Am. Miner. 82 (1997) 51.
[45] G. Grimvalli, Thermophysical Properties of Materials, North-Holland, Amsterdam, 1999.
[46] A. Reuss, Z. Angew. Math. Mech. 9 (1929) 49.
[47] W. Voigt, Lehrburch der Kristallphysik, Teubner, Leipzig, 1928.
[48] R. Hill, Proc. Phys. Soc. A 65 (1952) 349.
[49] R. Hill, J. Mech. Phys. Solids 11 (1963) 357.
[50] R. Hill, Proc. Phys. Soc. London 65 (1952) 396.
[51] D.H. Chung, W.R. Buessem, J. Appl. Phys. 38 (1967) 2010.
[52] M. Mattesini, M. Magnuson, F. Tasnádi, C. Höglund, I.A. Abrikosov, L. Hultman, Phys. Rev. B 79 (2009) 125122.
[53] S.F. Pugh, Philos. Magn. 45 (1954) 823.
[54] O.L. Anderson, J. Phys. Chem. Solids 24 (1963) 909.